ResearchGate

See discussions, stats, and author profiles for this publication at: https://www.researchgate.net/publication/44627980

Molecular dynamics simulations of the chain dynamics in monodisperse oligomer melts and of the oligomer tracer diffusion in an entangled polymer matrix

ARTICLE *in* THE JOURNAL OF CHEMICAL PHYSICS · MAY 2010

Impact Factor: 2.95 · DOI: 10.1063/1.3420646 · Source: PubMed

CITATIONS
14

READS
23

5 AUTHORS, INCLUDING:

Olivier Vitrac

French National Institute for Agricultural Res…

64 PUBLICATIONS **509** CITATIONS

SEE PROFILE

Available from: Olivier Vitrac
Retrieved on: 26 January 2016

Molecular dynamics simulations of the chain dynamics in monodisperse oligomer melts and of the oligomer tracer diffusion in an entangled polymer matrix

M. Durand,[1,a),b)] H. Meyer,[1] O. Benzerara,[1] J. Baschnagel,[1] and O. Vitrac[2,a),c)]
[1]*Institut Charles Sadron, CNRS, 23 Rue du Loess–BP 84047, 67034 Strasbourg Cedex 2, France*
[2]*UMR Génie Industriel Alimentaire, AgroParisTech Site de Massy, 1 Avenue des Olympiades, 91744 Massy Cedex, France*

(Received 11 February 2010; accepted 9 April 2010; published online 18 May 2010)

The apparent analogy between the self-diffusion of linear oligomers in monodisperse systems, 2 up to 32 monomers, and their tracer diffusion in an entangled polymer matrix of length 256 is investigated by molecular dynamics simulations at constant pressure. Oligomers and polymers are represented by the same coarse-grained (bead-spring) model. An analysis based on the Rouse model is presented. The scaling relationship of the self-diffusion coefficient D with the chain length N written as $D \propto N^{-\alpha}$ is analyzed for a wide range of temperatures down to the glass transition temperature T_g. Near T_g, the heterogeneous dynamics is explored by the self-part of the van Hove distribution function and various non-Gaussian parameters. For the self-diffusion in a monodisperse system a scaling exponent $\alpha(T) > 1$ depending on temperature is found, whereas for the tracer diffusion in an entangled matrix $\alpha = 1$ is obtained at all temperatures, regardless of the oligomer length. The different scaling behavior between both systems is explained by a different monomer mobility, which depends on chain length for monodisperse systems, but is constant for all tracers in the polymer matrix. © *2010 American Institute of Physics*. [doi:10.1063/1.3420646]

I. INTRODUCTION

In many technological areas, understanding the molecular diffusion mechanism in polymer materials is of significant concern in both qualitative and quantitative ways. The diffusion and rheological properties of linear and branched polymers depend on the scaling relationship of the polymer self-diffusivity and viscosity with molecular weight.[1] In formulated materials such as common polyolefins and polystyrenes, self-diffusion controls the loss of additives and consequently the lifetime of the processed material or the contamination of materials in contact (e.g., food, environment).[2] In this perspective, the development of predictive models of the diffusion coefficients of tracers could help the design of safer materials[3] and the assessment of the consumer's exposure to contaminants originating from polymer materials.[4]

For both self-diffusion of monodisperse melts and tracer diffusion of dispersed solutes in an entangled matrix (e.g. additives, polymer residues), the dependence between the molecular mass of the diffusing species (N) and its diffusion coefficient (D) must be elucidated.

For linear polymers, several theories have been related to experimental scaling relationships, such as $D \propto N^{-\alpha}$ with a scaling exponent α. For chains that are significantly shorter than the entanglement length N_e, polymer motion is expected to be controlled by the balance between friction forces, random forces, and entropic forces on each subunit. A scaling exponent $\alpha = 1$ is then foreseen, as predicted by the Rouse model.[5] The reptation model ($\alpha = 2$) predicts that very long chains in concentrated solutions or melts are constrained by their neighboring intertwined chains and that they can therefore diffuse only along their own contour. Literature data in melts were found consistent with $\alpha = 2.3$ (Ref. 1) based on several measurement techniques (including pulse-field gradient NMR) or $\alpha = 2.4$ (Ref. 6) based on measurements of the diffusion coefficient with pulsed-field gradient nuclear magnetic resonance. The discrepancies between the model and experiments have been related to additional mechanisms including constraint release, as inferred by neutron spin echo,[7] or fluctuations[8] of the virtual tube confining the diffusing polymer.

Experimental data for the self-diffusion of linear alkanes in monodisperse melts showed that the N dependence was stronger than predicted by Rouse theory and that it varied with temperature and pressure. In liquid n-alkanes with 8–60 carbons, Meerwall *et al.*[9] found values from $\alpha = 2.72$ down to $\alpha = 1.85$ when temperature was changed from 30 to 170 °C, and with the special case $\alpha = 2$ obtained at 130 °C. It was shown that the experimental results could be reconciled with $\alpha = 1$ by applying a static correction due to the excess free volume of the chain ends. The geometric effect associated with free volume was investigated for C_{60} and the thermal dependence of α was analyzed by molecular dynamics (MD) simulations for alkanes ranging between C_{16} and C_{60}.[10] Long term atomistic MD simulations of polyethylene melts led to the identification of a Rouse regime for chain lengths ranging approximately between C_{90} and C_{140} at 450 K.[11]

For small tracer molecules dispersed at very low concen-

[a)]Authors to whom correspondence should be addressed.
[b)]Electronic mail: manuel.durand@ics-cnrs.unistra.fr.
[c)]Electronic mail: olivier.vitrac@agroparistech.fr.

 © 2010 American Institute of Physics

tration in a host matrix of much longer chains, the possible variety of scaling exponents is even larger. In semicrystalline polyolefins (i.e. at solid state), α values much greater than 1 were found for additivelike molecules,[12] with values between 1.6 and 4 for temperatures ranging between 23 and 40 °C and for linear alkanes (between C_{12} and C_{18}), with values close to 2.[13] A similar range between $\alpha=2$ and 4.7 for temperatures ranging from 23 to 85 °C was obtained in a lightly cross-linked amorphous polyamide around or above the glass transition temperature (T_g).[14]

In polyolefin matrices the rapid slowing down of the tracer diffusion with N in the solid state of the matrix contrasts highly with its behavior in the molten (liquid) state. After extrapolation of diffusion coefficients to infinite dilution, a value of α close to 1 was inferred for n-alkanes (between C_{24} and C_{60}) in polyethylene melts at 180 °C.[6] Large α values above 4 are inferred from experimental gas and vapor values in poly(vinyl chloride),[15] polystyrene, and poly(methyl methacrylate) at 30 °C.[16] By comparison of similar tracers, α values lower than or equal to 1 are derived in natural rubber at room temperature.[17] Reference determinations of tracer diffusion of radiolabeled n-dodedecane and n-hexadecane in various elastomers at 25 °C (Ref. 18) gave an even lower mass dependence with a likely α value of 0.55 ± 0.07.

The discussion above exemplifies the wide spread of α values that were obtained from experiments. Some of the determined exponents are consistent with $\alpha=1$ of the Rouse model. This is the case for the self-diffusion of liquid alkanes in monodisperse melts or for the tracer diffusion of alkanes in polyethylene melts. However, most of the found exponents are completely different from $\alpha=1$. For instance, $\alpha=2$ is obtained for the diffusion of alkanes in polyethylene at solid state. Very large α values, close to 4, are ascertained for tracers in a polyamide around T_g and exponents smaller than 1 are found in various elastomers. Therefore, it seems that the tracer diffusion strongly depends on the properties of the matrix (e.g. semicrystalline, solid, or liquid). The commonly accepted exponent $\alpha=1$ of the Rouse model to describe the dynamics of short chains is therefore open to question. Moreover, it is sometimes argued that differences in density (free volume theory) could explain the spread of α values between polymers or between polymer states. However, for tracers much larger than the accessible voids the role of the renewal of the local environment on their diffusion is strongly limited and relaxation processes involving many-body correlations must be considered. Here, our aim is to obtain a better understanding of the complex experimental situation sketched above by performing MD simulations of a generic coarse-grained model to analyze the diffusion of oligomers in monodisperse systems and in an entangled polymer matrix at various temperatures down to T_g.

Coarse-grained polymer models have been used in the past to study the glass transition of polymer melts (for reviews, see, e.g., Refs. 19 and 20) and the crossover from nonentangled to entangled chain dynamics[21–23] where a Rouse-like exponent $\alpha \simeq 1$ is found for $N<N_e$, whereas a reptationlike exponent is determined for $N>N_e$. However, the validity of reptation theory is still fairly controversial, and simulations of coarse-grained model play an important role in this active field of research.[22,23] Other simulations based on bead-spring models aimed at probing the glass transition of undercooled polymer melts by using single molecule spectroscopy.[24,25] The influence of the size of spherical penetrants in a polymer matrix with a variable flexibility was also studied by a coarse-grained model,[26] and it has been shown that qualitatively similar results are obtained for purely repulsive and attractive bead-spring chains.[27]

However, to the best of our knowledge a MD study of the tracer diffusion in an entangled polymer host of a series of homolinear coarse-grained chains has not been carried out yet. Therefore, the aim of the present work is twofold: (i) to provide reference coarse-grained simulation data for the self-diffusion in monodisperse systems and tracer diffusion in a polymer matrix for a wide range of temperatures and linear tracers resembling polymer chains; (ii) to explore the origin of possible deviations from the Rouse theory at both the microscopic (purely viscous damping process) and macroscopic process scales ($D \propto N^{-\alpha}$).

The paper is organized as follows. The simulation procedure is detailed in Sec. II. The main properties of the Rouse theory are summarized in Sec. III along with criteria to test the theory. The results above T_g and in vicinity of T_g are presented in Sec. IV. The increasing role of heterogeneous dynamics on diffusion coefficients on approach to T_g is particularly highlighted. Finally, Sec. V summarizes the main findings and sketches future work.

II. SIMULATION DETAILS

A. Model

Oligomer and polymer segments were idealized at a coarse-grained scale by flexible, noncrystallizable, bead-spring models. Interactions between nonbonded monomers were represented by a truncated and shifted Lennard-Jones (LJ) potential with a cutoff radius corresponding to the minimum of the LJ potential,

$$U_{\mathrm{LJ}}^{\mathrm{rep}}(r) = \begin{cases} 4\epsilon\left[\left(\frac{\sigma}{r}\right)^{12} - \left(\frac{\sigma}{r}\right)^{6} + \frac{1}{4}\right] & \text{for } r \le r_{\min} \\ 0 & \text{else.} \end{cases} \quad (1)$$

All quantities are expressed in dimensionless LJ units. In this framework, lengths, energies, and temperatures are scaled by σ (monomer diameter), ϵ, and ϵ/k_B. For convenience, the Boltzmann constant k_B and monomer mass are set to 1. Time scale is expressed in units of $\tau=(m\sigma^2/\epsilon)^{1/2}$. Along the polymer chain, connected monomers are not subjected to a LJ potential but to a harmonic potential instead,

$$U_{\mathrm{bond}}(r) = \tfrac{1}{2}k(r-b_0)^2, \quad (2)$$

where $b_0=0.967$ is the average bond length between two monomers along the chain. Bonded monomers tend to slightly overlap because b_0 is smaller than the average bead distance imposed by the LJ potential. The spring stiffness $k=1111$ was chosen large enough to prevent chains from crossing each other. The incommensurability between the lengths imposed by the harmonic and the LJ potentials and

the intrinsic flexibility of the chains impede crystallization on cooling. Our model is very flexible as backfolding is only prevented by the LJ potential. The minimum angle between two neighboring bonds is approximately 60°.

B. Studied systems

Two types of systems were considered: monodisperse linear systems consisting of 3072 monomers and polydisperse linear systems consisting of a total of 12 288 monomers. As in our coarse-grained model a monomer has a unitary molecular mass, the molecular mass of each linear tracer is determined by its number of monomers, N. Oligomers of lengths $N=2(1536)$, 4 (768), 8 (384), 16 (192), 32 (96), and 64 (48) were considered in the monodisperse systems, where the figure in parentheses represents the number of chains. For the polydisperse systems, a long chain matrix of $N=256$ was considered with a small fraction of tracers in the same size range as studied for the monodisperse systems, $N=1(8)$, 2 (4), 4 (4), 8 (4), 16 (4), 32 (4), and 64 (4).[28] The tracer concentrations range from 1% to 4% which was low enough to avoid significant plasticization effects of the matrix.

C. Simulation procedure

The equations of motion were integrated using the velocity-Verlet algorithm with a time step of $\delta t=0.01$. Simulations were performed under isothermal and isobaric conditions (NpT ensemble) using a Langevin thermostat and a Berendsen barostat. The friction coefficient of the thermostat was set to $\gamma=0.1$ and the coupling parameter of the barostat to $\tau_p=1\times10^{-5}$. The initial configuration was generated at a density of $\rho=0.85$ corresponding to a standard polymer melt.[21] At $T=1.0$, the purely repulsive bead-spring melt has a pressure of $p\approx5$. This pressure was used throughout this work. The initial configuration is equilibrated under NpT conditions at $T=1.0$ and $p=5.0$ during $\tau_e=22\,000\tau$, which is sufficient for complete relaxation of the chain length $N=64$ (decorrelation time of the end-to-end distance is about $3\times10^3\tau$). The obtained configuration was used as a starting configuration for the long-time simulation at $T=1.0$. The equilibration was verified by ensuring that the density shows no drift and that all chains could translate on distances larger than their mean-square end-to-end distance R_e^2. Configurations at lower temperatures were obtained by cooling the last configuration from $T=1.0$ down to the desired temperature at constant pressure with a cooling rate of $\Gamma_T=2\times10^{-5}$. The obtained configuration was subsequently equilibrated as previously described for $T=1.0$. Note that the static properties of the flexible bead-spring model only weakly vary with the temperature. Re-equilibration at lower T is thus not a critical issue. Long-time simulations were finally performed for each temperature until the self-diffusive regime of the longest chains was reached [mean-square displacements (MSDs) greater than R_e^2]. At very low temperatures near T_g the dynamics was dramatically slowed down especially for long chains. At $T=0.3$, the self-diffusive regime of the whole matrix was not reached but it was possible to assess the diffusion of tracers shorter than the host chains. We checked that dynamical quantities calculated on subtrajectories gave the same result within the statistical error, and no aging effects were found.

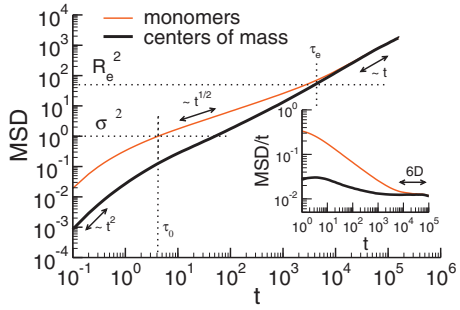

FIG. 1. Main figure: MSD of the monomers (thin line) and of the CM (thick line) of the chains for chain length $N=32$ at $T=1.0$. Intersection of the monomer MSD with horizontal dotted line at σ gives τ_0 and intersection of chain's CM MSD with dotted line at R_e^2 gives the relaxation time τ_e. Inset: MSD divided by t. The diffusion coefficient D is given by a plateau regime at long times.

III. THEORY AND DEFINITIONS

A. MSDs

For a given tracer of length N (either host or tracer), two MSDs are of particular significance to assess their translation dynamics over broad time scales t: the MSD of monomers, denoted g_0, and the MSD of the center of mass (CM), denoted g_3. They are defined as

$$g_0(t)=\frac{1}{n_cN}\sum_{k=1}^{n_c}\sum_{j=1}^{N}\langle[\mathbf{r}_{k,j}(t)-\mathbf{r}_{k,j}(0)]^2\rangle, \tag{3}$$

and that of the chain CM,

$$g_3(t)=\frac{1}{n_c}\sum_{k=1}^{n_c}\langle[\mathbf{R}_k(t)-\mathbf{R}_k(0)]^2\rangle, \tag{4}$$

where $r_{k,j}$ is the position of the monomer j in the kth tracer of length N (total number of tracers$=n_c$); $\mathbf{R}_k$ is the corresponding CM position. All positions were chosen relative to the CM reference frame of the whole system.

A typical evolution of $g_0(t)$ and $g_3(t)$ is depicted in Fig. 1 for a monodisperse system with $N=32$ at $T=1.0$. On short time scales, the monomers are uncorrelated so that $g_3\propto g_0/N$. The first ballistic regime ($\propto t^2$) ends as soon as the monomers feel the interaction with their neighbors. The connectivity leads to a characteristic subdiffusive regime $g_0\propto t^{\approx1/2}$. At long times the motion of the monomers relative to the CM of each chain becomes small and one reaches the freely diffusive regime where the diffusion coefficient can be obtained from the Einstein relation,

$$g_0(t)\overset{t\to\infty}{=}g_3(t)\overset{t\to\infty}{=}6Dt. \tag{5}$$

Characteristic times τ_0 and τ_e identified in Fig. 1 are determined when $g_0(t)$ equals σ^2 (for τ_0) and when $g_3(t)$ equals the mean-square end-to-end distance (R_e^2) of the chain (for τ_e).

B. Rouse model

The Rouse model was introduced by Rouse[5] in 1953 and has become a standard theoretical framework to analyze the dynamics of short nonentangled chains. It describes the Brownian motion of beads connected by (thermal) springs, neglecting excluded volume. In a dense melt, the effect of excluded volume is supposed to determine the friction coefficient (more subtle effects for long chains are described in Ref. 29). The Rouse model is solved via transformation to normal coordinates, the so-called Rouse modes, defined as

$$\mathbf{X}_p(t) = \frac{1}{N}\sum_{i=1}^{N} \mathbf{r}_i(t)\cos\left(\frac{\left(i-\frac{1}{2}\right)p\pi}{N}\right), \tag{6}$$

where $\mathbf{r}_i(t)$ is the position of monomer i of the chain. The mode p can be interpreted as a new variable describing subsegments of size N/p. For the pure Rouse model without excluded volume, the autocorrelation functions of these Rouse modes decay exponentially $\langle \mathbf{X}_p(t)\cdot\mathbf{X}_p(0)\rangle \propto \exp(-t/\tau_p)$ with relaxation times τ_p,

$$\tau_p = \frac{\xi_0 b^2}{12 k_B T}\left[\sin\frac{p\pi}{2N}\right]^{-2}, \tag{7}$$

where ξ_0 is the monomeric friction coefficient and b is the effective bond length defined by

$$R_e^2 = b^2(N-1). \tag{8}$$

The rouse times can be expressed as a function of the smallest relaxation time τ_{N-1},

$$\tau_p = \tau_{N-1}\left[\frac{\cos(\pi/2N)}{\sin(p\pi/2N)}\right]^2. \tag{9}$$

As the Rouse modes represent only a coordinate transformation, the MSD can be expressed exactly in terms of them,

$$g_0(t) = 6\frac{k_B T}{N\xi_0}t + 4\sum_{p=1}^{N}\langle \mathbf{X}_p^2(0)\rangle\left[1-\frac{\langle \mathbf{X}_p(t)\cdot\mathbf{X}_p(0)\rangle}{\langle \mathbf{X}_p^2(0)\rangle}\right]$$
$$= g_3(t) + g_2(t), \tag{10}$$

with

$$\langle \mathbf{X}_p^2(0)\rangle = \frac{b^2}{8N}\left[\sin\frac{p\pi}{2N}\right]^{-2}. \tag{11}$$

The first term of Eq. (10) is the zero mode component representing the CM motion $g_3(t)$ which predicts the diffusion coefficient, D, to be

$$D = \frac{k_B T}{N\xi_0} = \frac{g_3(t)}{6t} = \lim_{t\to\infty}\frac{g_0(t)}{6t}. \tag{12}$$

In practice, the displacement spectrum is assumed to be well sampled when a chain has moved over a distance greater than its own end-to-end distance R_e^2 (see Fig. 1). This condition is achieved for time scales $t > \tau_e$, where τ_e is defined by $g_3(\tau_e) = R_e^2$ so that

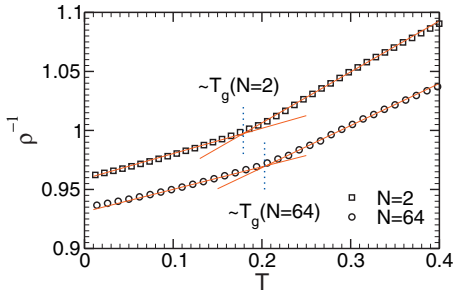

FIG. 2. Inverse density of a monomer as a function of temperature for monodisperse $N=2$ (squares) and $N=64$ (circles) systems. The lines are fits of the liquid and solid branches of the dilatometric data. The intersection of those lines determines the T_g of the system.

$$D = \frac{R_e^2}{6\tau_e}. \tag{13}$$

This implies

$$\tau_e = \frac{\xi_0 b^2 N(N-1)}{6k_B T} = \tau_0 N(N-1), \tag{14}$$

with τ_0 being the required time for a monomer to diffuse a distance comparable to the effective bond length b. According to Eq. (14), the long relaxation time τ_e can be assessed by the monomeric relaxation time τ_0.

IV. RESULTS AND DISCUSSION

This section details the results on both monodisperse and polydisperse systems at various temperatures. We start with the characterization of monodisperse systems (Secs. IV A–IV D), while the polydisperse systems are examined in Sec. IV E.

A. Chain length dependence of the glass transition temperature

The glass transition temperature T_g is derived from the variation in the specific volume ρ^{-1} on cooling. The results are plotted in Fig. 2 for two extreme cases: $N=2$ and $N=64$. T_g is defined as the intersection of straight lines extrapolated from the glassy and liquid states. We fit the lower-T branch (glassy state) and the high-T branch (liquid state) over the largest possible range of temperature and take the same interval in temperature for both branches.[30–39] Figure 3 shows that T_g increases with N and that the chain length dependence is compatible with the empirical Fox–Flory equation,

$$T_g = T_g^{\infty} - \frac{A}{N}, \tag{15}$$

which usually describes experimental data well (if the molecular weight is not too small[40]), although other forms have also been discussed recently.[41,42]

B. Relaxation dynamics of monodisperse systems: comparison with the Rouse model

In this section, the polymer dynamics is compared with the predictions of the Rouse theory, either through the Rouse

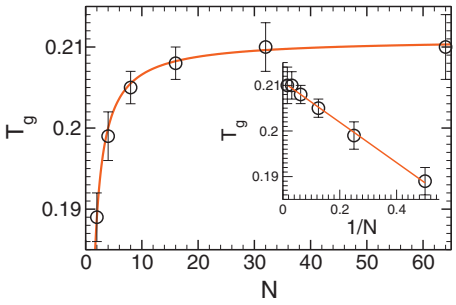

FIG. 3. Glass transition temperature T_g as a function of the chain length N. Error bars depict the standard deviation of 15 determinations. The inset displays T_g as a function of $1/N$. The line is a fit according to Eq. (15) with $T_g^{\infty} \simeq 0.211$ and $A \simeq 0.044$.

mode relaxation times τ_p [Eq. (9)] or through the MSD $g_2(t)$ [Eq. (10)]. Section IV C will address the scaling of the diffusion coefficient with N and T.

From the decay of the Rouse mode correlation function $C_{pp}(t)$, we determine the relaxation times τ_p by the condition $C_{pp}(\tau_p)=1/e$. For two extreme temperatures $T=1.0$ and $T=0.3$, Fig. 4 shows these relaxation times multiplied by $\sin^2(p\pi/2N)$ so that a constant should be expected if Rouse theory applied. To a first approximation, this is the case. However, the presentation chosen in Fig. 4 highlights deviations from Rouse behavior. We see that the points for different N/p are not perfectly horizontal, and that for the low temperature, the results for different chain lengths do no longer collapse onto a master curve. Such deviations are not unexpected. For $N/p<10$ the chain segments probed by the Rouse modes are small so that local features of the model and monomer caging at low T strongly influence the dynamics.[43]

At $T=0.3$, the Rouse times do not collapse as well as at $T=1$ and a faster relaxation of shorter chains relative to long ones is found. Here we argue that this effect is related to the N-dependence of T_g. At $T=0.3$, the system is sufficiently close to T_g such that an N-dependence of the mobility must be expected. We thus have to assume that the friction coefficient $\xi_0(T,N)$ depends on both chain length and temperature; we will come back to this point in Sec. IV C.

Let us now compare Rouse theory and simulation via the monomer MSD. Here we concentrate on the intermediate subdiffusive regime which reflects the impact of chain connectivity on the monomer dynamics (cf. Fig. 1). To highlight this regime we plot $g_2(t)=g_0(t)-g_3(t)$ [see Eq. (10)]. For

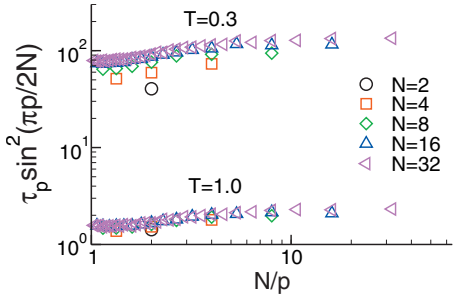

FIG. 4. Rouse times τ_p multiplied by $\sin^2(p\pi/2N)$ as a function of N/p for the monodisperse systems at $T=1.0$ (lower part of the figure) and at $T=0.3$ (upper part).

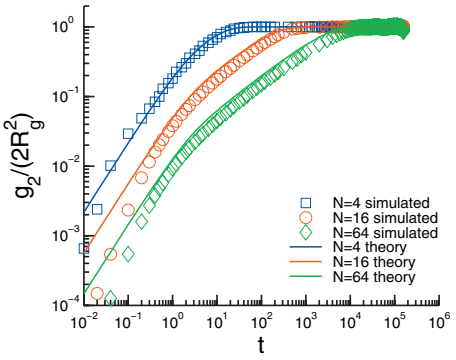

FIG. 5. $g_2(t)/(2R_g^2)$ from the simulation (symbols) and from Rouse theory (lines; see text for details) at $T=1.0$ and different chain lengths $N=4,16,64$.

large times, when the chains have completely relaxed and enter the free diffusion regime, the motion relative to the chain's CM is restricted to a finite value, $g_2(t\to\infty)=2R_g^2$ (R_g being the radius of gyration of a chain). Therefore, the ordinate in Figs. 5 and 6 is rescaled by the simulated or theoretical $2R_g^2$, which forces simulation and theory to agree at long times. The theoretical curves in the figures are obtained by assuming an exponential relaxation of the Rouse modes in Eq. (10) with τ_p and $\langle \mathbf{X}_p^2(0)\rangle$ given by Eqs. (9) and (11), respectively. The value of b^2 in Eq. (11) is determined from Eq. (8). We checked that the decay of the Rouse mode correlation function $C_{pp}(t)$ is approximately exponential for temperatures down to $T=0.3$. At $T=0.25$, a stretching is visible and for $T\leq 0.23$, a two-step decay occurs[44] but it is not discussed further here.

At $T=1$, Fig. 5 shows that theory and simulation are rather close for all chain lengths studied, if time is sufficiently outside the initial ballistic regime. Residual deviations may be traced back to the fact that the Rouse modes are not purely exponential and $\langle \mathbf{X}_p^2(0)\rangle$ does not fully agree with the Rouse prediction. At low temperature close to T_g, however, the deviations become more pronounced. Figure 6 reveals that the simulation data display a two-step increase which is not present in the theory. Such a two-step increase is extensively discussed in the literature (see, e.g., Refs. 19 and 20) and may be attributed to strong monomer caging which slows down the structural relaxation near the glass transition.[43] This effect is, of course, not contained in the Rouse theory.

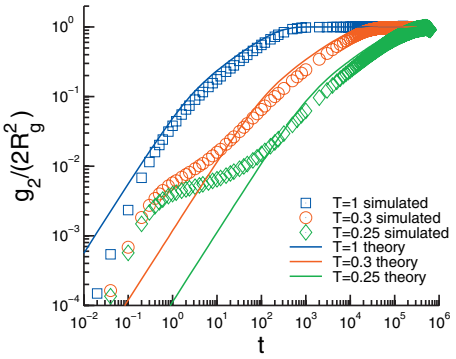

FIG. 6. $g_2(t)/(2R_g^2)$ obtained from simulation (symbols) and theory (lines) for $N=16$ at different temperatures $T=1.0,0.3,0.25$.

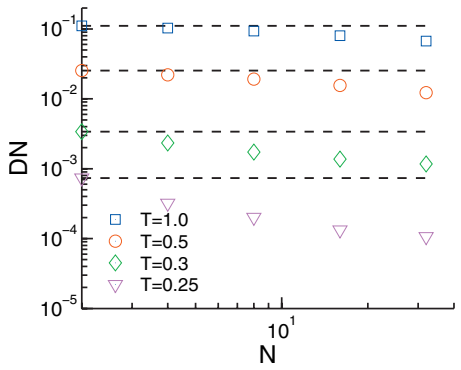

FIG. 7. DN as a function of N for monodisperse systems at $T=1.0$, 0.5, 0.3, and 0.25. The dashed black lines indicate the behavior according to the Rouse model.

Simulations of nonentangled chains[30,43–45] find both accord with Rouse predictions—e.g., the Rouse modes are (nearly) orthogonal for all t—and deviations from them—e.g., the Rouse modes are stretched with stretching exponents depending on the mode index and the MSD of the chain's CM increases sublinearly for intermediate times. The origin of these deviations is not fully understood. However, for short chains the relaxation time of a chain is not well separated from the (local) α-relaxation so that finite-N corrections to the Rouse behavior must be expected.[43] Moreover, even for long chains intermolecular interactions between the polymers are not completely screened on mesoscopic length scales, which may cause subdiffusive CM motion[46] or deviations from reptation theory[22] and lead to corrections to chain ideality.[29,47]

C. Diffusion coefficients of monodisperse systems

The Rouse theory predicts $D \propto 1/N$. To test this prediction for different temperatures, Fig. 7 plots DN as a function of N [with D obtained from Eq. (12) in the simulation]. At $T=1$, this "Rouse dependence" is rather well verified, despite systematic deviations which become larger with increasing N. This is expected as significantly longer chains are supposed to be slowed down by entanglements. The entanglement length of our flexible model is $N_e \approx 60$, and the chain lengths studied only show small precursor effects of entanglements. At lower temperature, the deviations from the $1/N$ dependence are more pronounced. Following the common experimental practice alluded to in Sec. I we introduce a T dependent scaling exponent α as

$$D \propto \frac{1}{N^{\alpha(T)}}. \tag{16}$$

Table I contains $\alpha(T)$ obtained by fitting the data of Fig. 7. It is seen that this apparent scaling exponent $\alpha(T)$ increases strongly with temperature from $\alpha(1.0) \simeq 1.1$ up to almost 2 at $T=0.25$. One could naively interpret this behavior as a crossover to reptation dynamics on cooling. However, a closer look at Fig. 7 reveals that the strongest increase in this chain length dependence is found for the shortest chains. At $T=0.25$, the slope of DN versus N actually decreases with increasing N, whereas reptation effects should be stronger for longer chains. Thus, there should be another explanation of this effect.

TABLE I. Values of exponent α and parameter a of the fit $D=aN^{-\alpha(T)}$ at each temperatures.

T	α	a
1.0	1.1	0.12
0.5	1.2	0.030
0.3	1.5	0.0047
0.25	1.9	0.0013

Figure 8 shows the same data as Fig. 7, but multiplied with the monomeric relaxation time $\tau_0(N,T)$ determined from the prescription $g_0(\tau_0)=\sigma^2$ (see Sec. III A). Now, a good data collapse is obtained for all temperatures. This shows that the increase in the apparent scaling exponent $\alpha(T)$ reflects only the stronger chain length dependence of the monomeric friction coefficient at lower temperatures, rather than a change in diffusion mechanism.

This also means that once the monomeric relaxation time τ_0 is known, one can estimate the diffusion coefficient D from Rouse theory according to Eq. (14). This feature is particularly interesting as the asymptotic self-diffusion coefficients could be approximated from short-time MD simulations without simulating up to the asymptotic regime (after using, e.g., Monte Carlo moves for equilibrating the start configuration).

Figure 9 shows the temperature dependence of $1/\tau_0$ for one chain length, $N=16$. Remarkably, we observed (not shown) that the dependence of $1/\tau_0$ and the one of D on the temperature are identical. The evolution of $1/\tau_0$ with T is shown as an Arrhenius plot for temperatures ranging from 0.23 to 1. A straight line was approximately obtained in the high-T region (from $T=1$ to 0.4). Near T_g, significant deviations from Arrhenius behavior occur. For the whole temperature range, the evolution is better described by an expression from mode coupling theory (MCT),[48]

$$1/\tau_0 \propto C(T-T_c)^{\gamma}, \tag{17}$$

from which we obtain $T_c=0.22$ and $\gamma=2.0$ [$T_g(N=16)=0.208$, see Fig. 3]. All data are appropriately fitted except the last point at $T=0.23$ for which the simulated $1/\tau_0$ is greater than the predicted one, but it is well known that

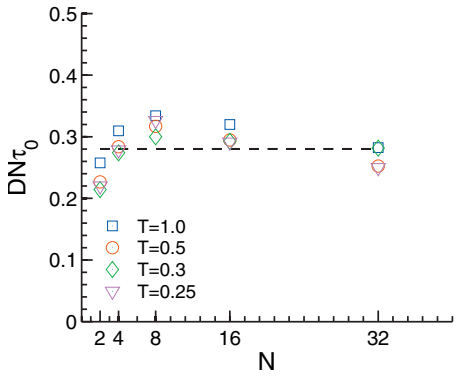

FIG. 8. $DN\tau_0$ as a function of N for temperatures $T=1.0-0.25$. The black dashed line is the mean value of all the $DN\tau_0$ points.

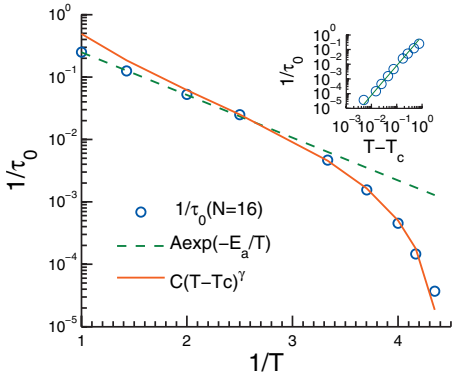

FIG. 9. Main figure: Arrhenius representation of the evolution of the inverse of the monomeric relaxation time $(1/\tau_0)$ with temperature for $N=16$ chains (circles). Temperature goes from 1 to 0.23. The dashed line is a fit to the Arrhenius law of the high-T region and the solid line is a MCT fit of the low-T region. Inset: $1/\tau_0$ as a function of T rescaled by the MCT temperature T_c.

Eq. (17) does not hold too close to T_c (see, e.g., Ref. 19).

Finally, we test the chain length dependence in an Arrhenius plot. Just plotting the raw data $1/\tau_0$ versus $1/T$ gives a strong shift of the data for different chain lengths (not shown), which is not a surprise after the results of the Rouse mode relaxation times (Fig. 4) and diffusion coefficient (Fig. 7). As we have already concluded that the proximity to the T_g changes the mobility, we renormalize the temperature axis with respect to $T_g(N)$, plotting a modified Arrhenius expression, Eq. (18),

$$1/\tau_0 = A\,\exp\left(-\frac{BT_g(N)}{T}\right). \tag{18}$$

The result in Fig. 10 shows a reasonable collapse onto a master curve. The longest chain length ($N=32$), however, deviates systematically to smaller values. We conclude that for the short oligomers, the correction because of the proximity to T_g is important, whereas for the longer chains, other effects, probably entanglements, are responsible for a different scaling behavior.

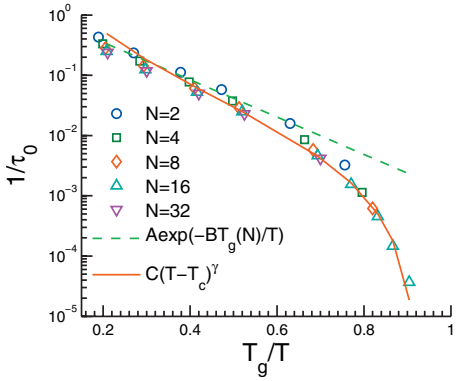

FIG. 10. Arrhenius representation of $1/\tau_0$ for the different chain lengths but rescaled by T_g. The dashed line is a fit to Arrhenius law and the line is an MCT fit for low temperatures.

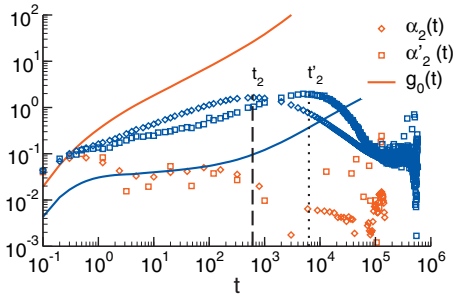

FIG. 11. Non-Gaussian parameter $\alpha_2(t)$ (diamonds), modified non-Gaussian parameter $\alpha_2'(t)$ (squares) and monomer MSD (lines) at temperatures $T=1.0$ (light color) and $T=0.23$ (deep color). The vertical dashed and dotted lines indicate respectively the peak times t_2 and t_2' of $\alpha_2(t)$ and $\alpha_2(t')$.

D. Dynamics near T_g

As temperature approaches T_g, many studies suggest that the dynamics becomes heterogeneous. This behavior was studied using the standard non-Gaussian parameters,

$$\alpha_2(t) = \frac{3}{5g_0(t)^2}\frac{1}{N_p}\sum_{i=1}^{N_p}\langle|\mathbf{r}_i(t)-\mathbf{r}_i(0)|^4\rangle - 1, \tag{19}$$

and a modified non-Gaussian parameter introduced in Ref. 49,

$$\alpha_2'(t) = \frac{g_0(t)}{3}\frac{1}{N_p}\sum_{i=1}^{N_p}\left\langle\frac{1}{|\mathbf{r}_i(t)-\mathbf{r}_i(0)|^2}\right\rangle - 1. \tag{20}$$

For Gaussian distributed displacements Eqs. (19) and (20) vanish. Positive values of α_2 and α_2' indicate that the monomers have moved farther in time t than expected for Gaussian displacements. The non-Gaussian parameters and $g_0(t)$ are plotted in Fig. 11 for the monodisperse system $N=16$ at two different temperatures $T=1.0$ ($\gg T_g$) and $T=0.23$ (close to T_g). At high temperature, the non-Gaussian parameters remained very small for all times. Near T_g, $g_0(t)$ exhibits a plateau regime following the short-time ballistic regime. The non-Gaussian parameters are significant and confirm the presence of non-Gaussian (correlated) displacements, which are responsible for the dramatic slowing down of the monomer motions. A detailed analysis of the displacements was performed by calculating the radial distribution function $P(r;t)$. The latter is related to the self-part of the van Hove correlation function $G_s(r,t)$ by[49]

$$P(\ln r;t) = 4\pi r^3 G_s(r,t) \tag{21}$$

and

$$G_s(\mathbf{r},t) = \frac{1}{N}\sum_{i=1}^{N}\langle\delta([\mathbf{r}_i(t)-\mathbf{r}_i(0)]-\mathbf{r})\rangle. \tag{22}$$

$G_s(r,t)$ is plotted on a semilog scale in Fig. 12 for the monodisperse system with $N=16$ at $T=1.0$ and $T=0.23$. The theoretical distribution corresponding to a Gaussian with zero mean and a variance equal to $g_0(t)$ is also represented. The Gaussian shape is well verified at high temperatures and at all time scales. By contrast at $T=0.23$, a bimodal shape is identified on intermediate time scales ($t \simeq t_2$). The position of the second maximum coincides with the monomer diameter.

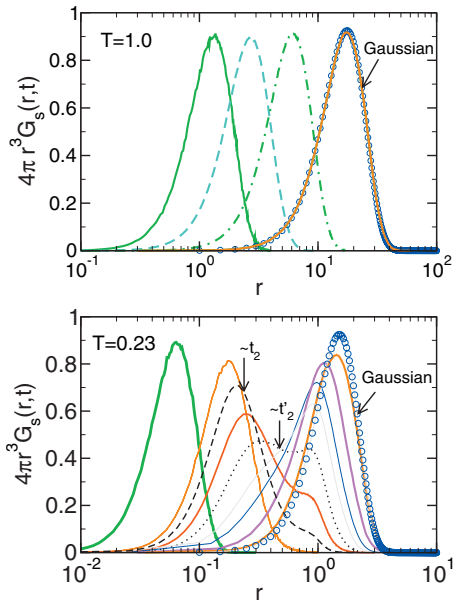

FIG. 12. Upper panel: Probability distributions functions at high temperature for times $t=10$, 100, 1000, and 10 000 (from the left to the right) for chain length $N=16$. For the last time we also drew in grey circles the theoretical expression of the Gaussian. Lower panel: Probability distributions functions at $T=0.23$ for times $t=0.1$, 10, 600, 2500, 6000, 10 000, 25 000, 50 000, and 100 000.

At $t \simeq t_2'$, both modes are equal, suggesting two coexisting populations: a caged one and a mobile one beyond a bead diameter as described in Refs. 49 and 50. For $t > t_2'$, the caged population vanishes progressively and the long-term distribution converges finally toward a Gaussian.

E. Tracer diffusion of oligomers in a long chain matrix

Multiconstituent mixtures consist in a matrix of long chains mixed with smaller chains. Two types of configurations were tested: bidisperse ones with only a single tracer and polydisperse systems with several tracers of different chain lengths. Bidisperse systems were mainly used to verify that the presence of tracers did not influence the matrix relaxation and structure factor. While the overall tracer concentration remained low, polydisperse systems contributed to reduce the computational effort for a large number of tracers. In addition, in the polydisperse system, all tracers feel exactly the same pressure. (Chain length dependent density or pressure corrections, which are always present for monodisperse systems, need not to be considered.) The glass transition temperature is not affected by the presence of the tracers; it was extrapolated from Eq. (15) to 0.211.

In analogy to the discussion of Sec. IV B, we calculate the Rouse mode relaxation times and the MSD of the tracers. Figure 13 shows the Rouse mode relaxation times multiplied by $\sin^2(p\pi/2N)$. The same N/p dependent deviations occur as for the monodisperse systems in Fig. 4. However, no N dependent shift is seen, regardless of temperature. This supports our interpretation of the previous sections that the monomeric mobility governs the temperature dependence. In the matrix system, this monomeric mobility is dominated by the matrix and is thus the same for all constituents.

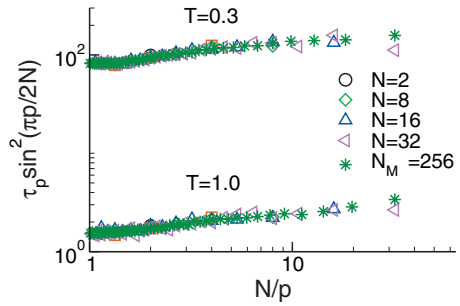

FIG. 13. Rouse times τ_p multiplied by $\sin^2(p\pi/2N)$ for all the tracer chain lengths and the matrix at temperatures $T=1.0$ and $T=0.3$.

The MSD derived from the Rouse modes, Eq. (10), were also compared with the simulated $g_2(t)$ for different temperatures and tracer lengths (not shown). The differences are similar to those found for the monodisperse case in Figs. 5 and 6.

Diffusion coefficients of tracers in a polymer host were obtained in a similar fashion as self-diffusion coefficients of monodisperse systems, from either the MSD of the CM or the relaxation time [see Eq. (13)],

$$D = \frac{g_3(\tau_r)}{6\tau_r}, \tag{23}$$

where $\tau_r = 3\tau_e$. (The factor "3" ensures that D is really determined in the diffusive regime for all chain lengths of the tracers.)

The chain length dependence shown in Fig. 14 is in remarkable agreement with the Rouse exponent $\alpha=1$ over the whole range of tracers studied and for all temperatures. This result differs strongly from the monodisperse systems where a temperature dependence of α was observed. This finding is completely consistent with the previous interpretation that in the polydisperse system, all tracers have the same monomeric relaxation time which depends only on temperature, but not on chain length any more. Similar observations have been made recently for experiments of alkanes in polyethylene.[6]

Estimated diffusion coefficients of tracers in a polymer host scaled with chain length are displayed as an Arrhenius plot in Fig. 15. For the high-T region (T ranged between 1.0 and 0.4) D follows an Arrhenius law, whereas a MCT law is

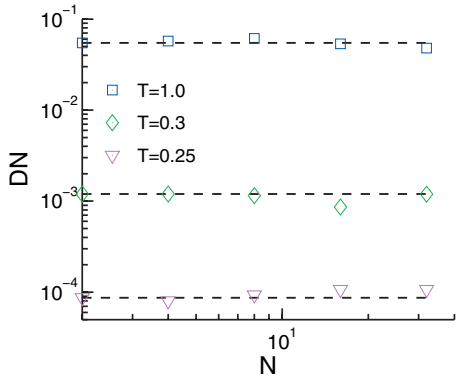

FIG. 14. Diffusion coefficient of the tracers multiplied by N as a function of N for temperatures $T=1.0$ down to $T=0.25$.

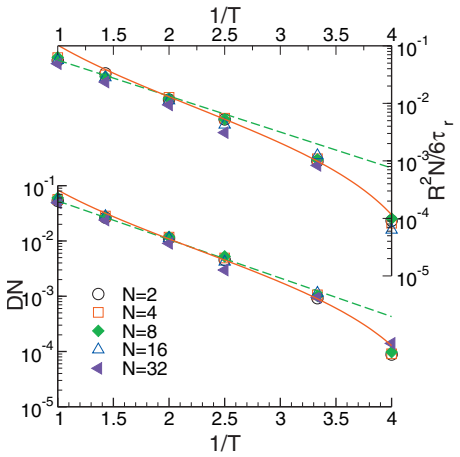

FIG. 15. Arrhenius representation of the evolution of the diffusion coefficient multiplied by N of tracers in $N_M=256$ matrix with the temperature. Upper panel: DN obtained from relaxation time τ_r. Lower panel: DN determined from the MSD. The dashed lines are fits to Arrhenius law for the high-T region and lines represent MCT fits for lower temperatures.

found more appropriate at lower temperatures near T_g. These results demonstrate that the asymptotic translation mechanism associated with the tracer diffusion among long chains and the one associated with its self-diffusion counterpart in monodisperse systems are very similar. Nevertheless, the diffusion coefficients in the entangled matrix were much slower for the polydisperse case especially for very short chains. This behavior is related to the relaxation time τ_0 which is governed by the matrix dynamics.

The coupling between the host relaxation and tracer diffusion is illustrated in Fig. 16 by plotting the monomer MSD for $N=2$ and 16 at $T=0.25$ for both monodisperse and polydisperse ($N_M=256$) systems. For the polydisperse systems, a short plateau regime for $t\simeq 1$ to $\simeq 30$ was clearly visible and confirmed that the whole system was close to its T_g. On intermediate time scales, it is worth to notice that the MSD for $N=16$ were not distinguishable between monodisperse and polydisperse systems. A separation occurred only after $g_0=R_g^2$ as the chain relaxation (τ_e) occurs earlier in the monodisperse case. For very short tracer lengths, the influence of the matrix is even stronger. In the special case of $N=2$ the two systems separated immediately after the ballistic regime.

The comparison between monodisperse and polydisperse systems is completed in Fig. 17 by the evolution of the non-

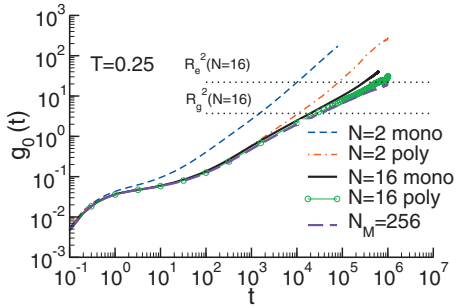

FIG. 16. Monomers MSD g_0 of monodisperse $N=2,16$ chains and polydisperse ones at $T=0.25$. The horizontal dotted lines are R_e^2 and R_g^2 of $N=16$ chains.

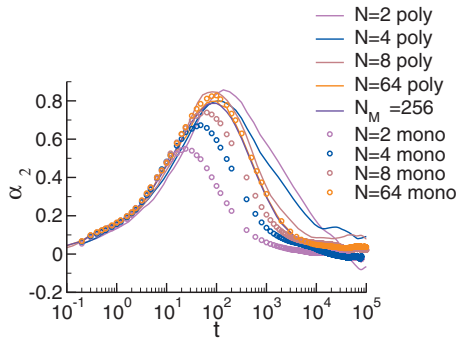

FIG. 17. Non-Gaussian parameter $\alpha_2(t)$ at $T=0.25$ for $N=2,4,8,64$ monodisperse chains represented by the symbols and for tracers $N=2,4,8,64$ in the polydisperse system symbolized by lines.

Gaussian parameter α_2 [Eq. (19)] at $T=0.25$ for $N=2,4,8,64$. Increasing the chain length leads to a shift of the maximum of the non-Gaussian behavior for monodisperse systems, while it had no effect for polydisperse systems. As this maximum is related to the monomeric relaxation time, these results confirm the crucial role of the host matrix on the dynamics of tracer on short and intermediate time scales.

V. CONCLUSIONS

We presented results based on MD simulations of the dynamics of oligomers in monodisperse systems and in an entangled matrix. Our simulations were run in the NPT ensemble and results are compared to the Rouse model. The dynamical properties were analyzed from high temperature down to the glass transition temperature and for different chain lengths of the oligomers ($N=2$ to $N=32$).

For monodisperse systems, the theoretical prediction for the dependence of the Rouse times on p (see Fig. 4) holds true only in a first approximation. Deviations are found at all temperatures. The study of the MSDs of monomers relative to their CM g_2 also shows deviations from the model (see Figs. 5 and 6). These results highlight the fact that the relation between monomer and chain diffusion is not as obvious as described by the Rouse model. We also determined the dependence of the chain diffusion coefficient (D) on chain length [given by Eq. (12)]. In agreement with previous experiments[9] and all atom simulations,[10] we found a power law dependence, $D\propto N^{-\alpha}$, with an apparent exponent α depending on temperature instead of $\alpha=1$ foreseen by the Rouse model. However, the Rouse model prediction ($\alpha=1$) can be recovered by introducing a monomer relaxation time which is related to the chain length dependence of the glass transition temperature.

For the oligomer dynamics in an entangled melt, the same deviations from the Rouse model were observed for the Rouse times and the MSD. Interestingly, the dependence of the tracer diffusion coefficient on chain length is given by $\alpha=1$ (Fig. 14). On the contrary to monodisperse systems, the same monomer relaxation time τ_0 is found for all the tracers because τ_0 is imposed by the matrix. This result is in very good agreement with a recent experimental work.[6]

Despite this agreement, our simulations do not shed light on the molecular mechanism which is responsible for the

large spread of α values found experimentally (see Sec. I). We speculate that the underlying mechanism could be related to the rigidity of the matrix. Therefore, work in progress aims at studying the tracer dynamics in more constrained systems such as semicrystalline and rigid matrices.

ACKNOWLEDGMENTS

Financial support by the CPR COPOLA is gratefully acknowledged. We are grateful to the INRA MIGALE bioinformatics platform (http://migale.jouy.inra.fr) for providing computational resources.

[1] T. P. Lodge, Phys. Rev. Lett. **83**, 3218 (1999).
[2] O. Vitrac, J. Lézervant, and A. Feigenbaum, J. Appl. Polym. Sci. **101**, 2167 (2006).
[3] O. Vitrac and M. Hayert, Chem. Eng. Sci. **62**, 2503 (2007).
[4] O. Vitrac and J.-C. Leblanc, Food Addit. Contam. **24**, 194 (2007).
[5] P. E. Rouse, J. Chem. Phys. **21**, 1272 (1953).
[6] E. D. von Meerwall, H. Lin, and W. L. Mattice, Macromolecules **40**, 2002 (2007).
[7] M. Zamponi, A. Wischnewski, M. Monkenbusch, L. Willner, D. Richter, A. Likhtman, G. Kali, and B. Farago, Phys. Rev. Lett. **96**, 238302 (2006).
[8] M. Doi, J. Polym. Sci., Part B: Polym. Phys. **21**, 667 (1983).
[9] E. von Meerwall and S. Beckman, J. Chem. Phys. **108**, 4299 (1998).
[10] V. Harmandaris, M. Doxastakis, V. Mavrantzas, and J. Theodorou, Chem. Phys. **116**, 436 (2002).
[11] V. Harmandaris, V. Mavrantzas, D. Theodorou, M. Kroger, J. Ramirez, H. Ottinger, and D. Vlassopoulos, Macromolecules **36**, 1376 (2003).
[12] J. Lezervant, O. Vitrac, and A. Feigenbaum, in Foodsim '2006: Fourth International Conference on Simulation and Modelling in the Food and Bio-Industry, edited by P. Masi and G. Toraldo, 2006, pp. 75–79.
[13] O. Vitrac, A. Mougharbel, and A. Feigenbaum, J. Food Eng. **79**, 1048 (2007).
[14] K. Kwan, C. Subramaniam, and T. Ward, Polymer **44**, 3061 (2003).
[15] A. R. Berens, Pure Appl. Chem. **53**, 365 (1981).
[16] A. R. Berens and H. Hopfenberg, J. Membr. Sci. **10**, 283 (1982).
[17] V. Stannett, W. Koros, D. Paul, H. Lonsdale, and R. Baker, *Recent Advances in Membrane Science and Technology* (Dekker, New York/Springer, Berlin, Heidelberg, 1974), Vol. 32, Chap. 2, p. 69.
[18] S. P. Chen and J. D. Ferry, Macromolecules **1**, 270 (1968).
[19] J. Baschnagel and F. Varnik, J. Phys.: Condens. Matter **17**, R851 (2005).
[20] J. L. Barrat, J. Baschnagel, and A. Lyulin, "Molecular dynamics simulations of glassy polymers," Soft Matter (in press), doi:10.1039/b927044b.
[21] K. Kremer and G. S. Grest, J. Chem. Phys. **92**, 5057 (1990).
[22] A. E. Likhtman, J. Non-Newtonian Fluid **157**, 158 (2009).
[23] S. K. Sukumaran and A. E. Likhtman, Macromolecules **42**, 4300 (2009).
[24] R. A. Vallée, W. Paul, and K. Binder, J. Chem. Phys. **127**, 154903 (2007).
[25] R. A. Vallée, M. V. der Auweraer, W. Paul, and K. Binder, EPL **79**, 46001 (2007).
[26] J. Budzien, J. D. McCoy, D. Rottach, and J. G. Curro, Polymer **45**, 3923 (2004).
[27] J. V. Heffernan, J. Budzien, A. T. Wilson, R. J. Baca, V. J. Aston, F. Avila, J. D. McCoy, and D. B. Adolf, J. Chem. Phys. **127**, 144711 (2007).
[28] Tests with a matrix $N=64$ and tracers $N=1(8)$, 2 (4),4 (4), and 16 (4), as well as bidisperse systems have also been performed. No significant differences to the polydisperse systems have been observed and the description in this paper refers to the polydisperse system of matrix length $N=256$.
[29] H. Meyer, J. P. Wittmer, T. Kreer, P. Beckrich, A. Johner, J. Farago, and J. Baschnagel, Eur. Phys. J. E **26**, 25 (2008).
[30] W. Paul and G. D. Smith, Rep. Prog. Phys. **67**, 1117 (2004).
[31] J. Buchholz, W. Paul, F. Varnik, and K. Binder, J. Chem. Phys. **117**, 7364 (2002).
[32] K. Binder, J. Baschnagel, and W. Paul, Prog. Polym. Sci. **28**, 115 (2003).
[33] A. V. Lyulin, N. K. Balabaev, and M. A. J. Michels, Macromolecules **36**, 8574 (2003).
[34] A. V. Lyulin, B. Vorselaars, M. A. Mazo, N. K. Balabaev, and M. A. J. Michels, Europhys. Lett. **71**, 618 (2005).
[35] A. Soldera and N. Metatla, Phys. Rev. E **74**, 061803 (2006).
[36] N. Metatla and A. Soldera, Macromolecules **40**, 9680 (2007).
[37] B. Schnell, Ph.D. thesis, University of Strasbourg, 2006.
[38] K. Vollmayr, W. Kob, and K. Binder, J. Chem. Phys. **105**, 4714 (1996).
[39] K. Vollmayr, W. Kob, and K. Binder, J. Chem. Phys. **54**, 15808 (1996).
[40] G. B. McKenna, in *Comprehensive Polymer Science*, edited by C. Booth and C. Price (Pergamon, New York, 1986), Vol. 2, pp. 311–362.
[41] J. Hintermeyer, A. Herrmann, R. Kahlau, C. Goiceanu, and E. A. Rösler, Macromolecules **41**, 9335 (2008).
[42] A. L. Agapov and A. P. Sokolov, Macromolecules **42**, 2877 (2009).
[43] S. H. Chong, M. Aichele, H. Meyer, M. Fuchs, and J. Baschnagel, Phys. Rev. E **76**, 051806 (2007).
[44] C. Bennemann, J. Baschnagel, W. Paul, and K. Binder, Comput. Theor. Polym. Sci. **9**, 217 (1999).
[45] M. Brodeck, F. Alvarez, A. Arbe, F. Juranyi, T. Unruh, O. Holderer, J. Colmenero, and D. Richter, J. Chem. Phys. **130**, 094908 (2009).
[46] M. Zamponi, A. Wischnewski, M. Monkenbusch, L. Willner, D. Richter, P. Falus, B. Farago, and M. Guenza, J. Phys. Chem. B **112**, 16220 (2008).
[47] J. P. Wittmer, P. Beckrich, H. Meyer, A. Cavallo, A. Johner, and J. Baschnagel, Phys. Rev. E **76**, 011803 (2007).
[48] S.-H. Chong and M. Fuchs, Phys. Rev. Lett. **88**, 185702 (2002).
[49] E. Flenner and G. Szamel, Phys. Rev. E **72**, 011205 (2005).
[50] S. Peter, H. Meyer, and J. Baschnagel, Eur. Phys. J. E **28**, 147 (2009).